ISSN: 2414-1895 DOI: 10.6919/ICJE.202501_11(1).0003

Characteristics of Shale Gas Reservoirs and Multi-scale Transport Mechanisms

Chenxing Wang

Sinopec Xinan Oilfield Service Corporation Downhole Operation Company, Deyang, 618000, China

Abstract

The shale gas reserves in our country are extremely abundant and possess considerable exploitation potential. The shale reservoir is highly compact. To obtain industrial production, the staged fracturing technology of horizontal wells is required. After the fracturing operation, a highly complex fracture network will form in the transformed area. These fracture networks mainly consist of artificial fractures and the natural fractures connected to them, providing excellent flow channels for gas flow. The vast majority of the pores in the shale reservoir are mainly nanoscale pores. The shale gas occurring in shale mainly exists in the forms of free and adsorbed states. The flow of shale gas in the reservoir differs from that of gas in conventional reservoirs. The flow of gas in shale encompasses multiple migration mechanisms such as viscous flow, diffusion, desorption, and slippage. Through research in this paper, it is found that in nanoscale pore diameters, the surface diffusion of gas is very obvious. As the pore size increases, the effects of viscous flow, slippage, and Knudsen diffusion intensify. In large pores, the effect of viscous flow dominates, followed in sequence by the slippage effect, Knudsen diffusion, and surface diffusion.

Keywords

Shale Gas; Fracture Network; Nano-Pores; Knudsen.

1. Research on Multi-scale Migration Mechanisms of Shale Gas

The flow of shale gas within the reservoir is categorized into three phases: ① the flow from nanopores to natural fractures; ② the flow from natural fractures to artificial fractures; ③ the flow process from artificial fractures to wellbores. As the pore sizes vary significantly during different flow processes, the flow patterns also exhibit considerable differences. To establish more precise flow patterns and production models for shale gas reservoirs, a more meticulous comprehension of the flow mechanisms of shale gas under different pore sizes is requisite.

In this article, the migration of free gas and adsorbed gas during the production of shale gas is primarily considered, encompassing a total of two categories and five migration mechanisms, specifically including:

(1) free gas migration

①viscous flow,②slip flow,③Knudsen diffusion

(2) adsorbed gas migration

①adsorbed gas desorption,②dsorbed gas surface diffusion

For shale gas, the aforementioned five migration mechanisms coexist, and they mutually influence and restrict one another. Pore size, pressure, and temperature are also factors influencing the migration of shale gas, with the extent of influence being characterized by the Knudsen number. The

ISSN: 2414-1895 DOI: 10.6919/ICJE.202501_11(1).0003

Knudsen number Kn is defined as the ratio of the average free path of gas λ to the pore throat size d, and it is extensively utilized as a dimensionless quantity to determine whether the fluid is suitable for the continuous assumption. The definition expression of the Knudsen number is as follows:

$$K_{\mathrm{n}} = \frac{k_{\mathrm{B}} T}{\sqrt{2}\pi\delta^2 p} \cdot \frac{2}{r} \tag{1}$$

Kn--Knudsen number, dimensionless,

λ--average molecular free path, nm,

d--pore throat diameter,nm,

kB--Boltzmann constant,1.3805×10-^{23}J/K,

T--temperature,K;

Δ--diameter of gas molecule collisions,m.

According to the value of Knudsen number, gas flow patterns can be divided into four categories (Figure 1): (1) continuous flow; (2) slip flow; (3) transition flow; and (4) free molecular flow.

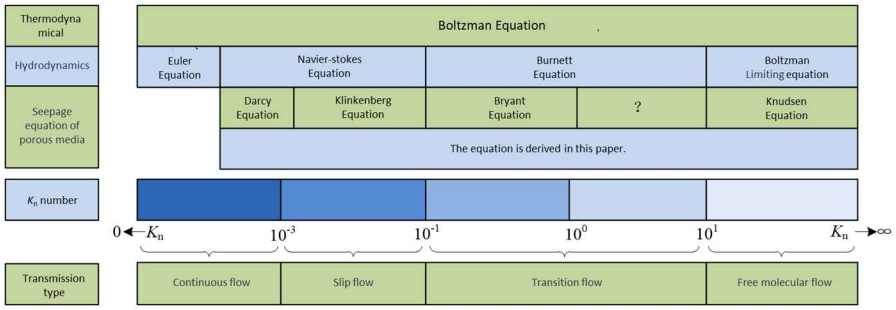

Figure 1. Classification of flow regimes and governing equations for each flow regime (modified from Shi et al.) [5]

Through research, it can be discerned that the flow patterns of shale gas are complex and diverse. As depicted in Figure 1, if each flow pattern possesses a distinct seepage model, considering all flow patterns separately and establishing seepage equations would render the calculation highly intricate, and the coupling issues among different seepage models would also need to be taken into account. Based on this issue, Adzumi, based on experimental studies, proposed a method of describing the permeability of the shale matrix using a unified equation and introduced the contribution coefficient ε, dividing the total flow into two parts, namely the viscous flow and the free molecule correction form. The expression is as follows:

$$N_{\mathrm{Tol}} = N_{\mathrm{Viscous}} + \varepsilon N_{\mathrm{Free}} \tag{2}$$

Mohammad et al., based on the research of Adzumi, divided the mass flow into two parts, namely the superimposed form of viscous flow and molecular free flow, and its expression is as follows:

$$N_{\mathrm{Tol}} = (1\text{-}\varepsilon)\ N_{\mathrm{Viscous}} + \varepsilon N_{\mathrm{Free}} \tag{3}$$

ISSN: 2414-1895 DOI: 10.6919/ICJE.202501_11(1).0003

$$\varepsilon = C_A[1-\exp(\frac{-K_n}{K_{nViscous}})]^S \tag{4}$$

Ntol--The total mass flux,kg/(s·m^2),

Nviscose--The continuous flow mass flux,kg/(s·m^2),

Nfree--The free molecular flow mass flux,kg/(s·m^2),

ε--The contribution coefficient, dimensionless, with the value range of 0.7 to 1,

CA--The constant, dimensionless,typically taken as 1,

KnViscous--The Knudsen number at which the transition from continuous flow to quasi-diffusion flow begins, typically taken as 0.3,

S--The constant, typically taken as 1.

The free and adsorbed states are the primary occurrence states of shale gas in shale reservoirs. In the model of this paper, the viscous flow, slip effect and Knudsen diffusion of shale gas are taken into account. The adsorbed shale gas undergoes surface diffusion and desorption, and corresponding mass transfer equations are established respectively. According to the study of the seepage models proposed by other scholars, a contribution coefficient ε is introduced into the seepage model in this paper, and different transmission mechanisms are superimposed to obtain a shale gas apparent permeability model that uniformly describes the multi-flow state mass transfer process.

1.1 The Migration Mechanism of Free Gas

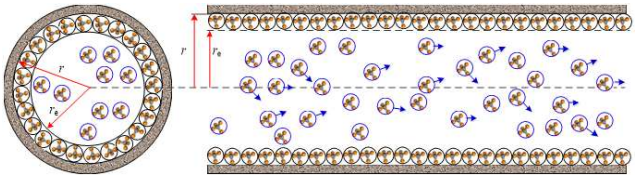

Figure 2. Schematic Illustration of Viscous Flow (The blue arrows represent the gas molecules undergoing viscous flow transportation)

When the Knudsen number is much less than 1, that is, when the average free path of motion of shale gas is far less than the pore diameter d, in this situation, the collisions of shale gas molecules with the surface of shale pores are relatively few. The majority of gas molecule movements are influenced by molecular forces, and the gas is dominated by continuous flow. Hence, the mass transfer equation of viscous flow is employed for description.

$$\begin{aligned} J_{vicious} &= -\rho\cdot\frac{1}{8\mu}(r-d_m\cdot\frac{p}{p+p_L})^2\cdot\nabla p \\ &= -\rho\cdot\frac{k_D}{8\mu}(1-\frac{d_m}{r}\cdot\frac{p}{p+p_L})^2\cdot\nabla p \end{aligned} \tag{5}$$

Jvicious--Mass flow rate of viscous flow,kg/(m^2·s),

ρ--Gas density,kg/m^3,

r--Effective flow radius corresponding to capillaries of different sizes,m,m,

μ--Gas viscosity,Pa·s,

p--Pore pressure,Pa,

∇ --Symbol of pressure gradient operator,

kD--Intrinsic permeability,m^2.

ISSN: 2414-1895 DOI: 10.6919/ICJE.202501_11(1).0003

1.2 The Slippage Effect

The slippage effect is mainly characterized by the increase in collisions between gas molecules and the pore wall due to the reduction in the scale of shale pores, such that the velocity of shale gas near the pore wall is no longer zero. Hence, at small scales, when $10^{-3} < Kn < 10^{-1}$, the free path of gas molecules increases and is comparable to the pore diameter. Under this condition, the slippage effect of the gas is mainly taken into account, as depicted in Figure (3).

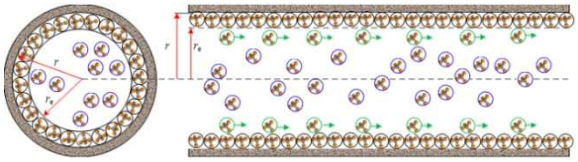

Figure 3. Schematic Diagram of the Slip Effect (Green arrows represent gas molecules undergoing slip effect transmission)

Typically, we employ Javadpour's model to compute the slip coefficient. Subsequently, the dimensionless slip coefficient F is introduced to rectify the slip effect of nanopores, obtaining the modified form of permeability:

$$\begin{aligned} k_{slip} &= k_D \cdot (1+F) \\ &= k_D \cdot [1+(\frac{8\pi RT}{M})^{0.5} \cdot \frac{\mu}{p_{avg} r} \cdot (\frac{2}{\alpha}-1)] \end{aligned} \tag{6}$$

F--The slip coefficient corresponding to the effective flow radius of capillaries of different sizes, dimensionless,

R--The gas constant,J/(mol·K),

T--Temperature,K,

M--Molar mass,kg/mol,

pavg--Average pressure, which is the average pressure at the inlet and outlet in a circular single tube,Pa,

α--Tangential momentum adjustment coefficient, dimensionless, with a value ranging from 0 to 1.

1.3 Knudsen Diffusion

When Kn > 10, the pore throat diameter within the shale matrix reduces, and the average free path of molecules increases under low-pressure conditions, thereby resulting in a notable increase in the contact between gas molecules and the rock wall surface. However, the direct mutual collisions among molecules become significantly less, and each molecule becomes more independent. At this point, this situation is typically termed Knudsen diffusion. The Knudsen diffusion mass transport equation can be formulated as:

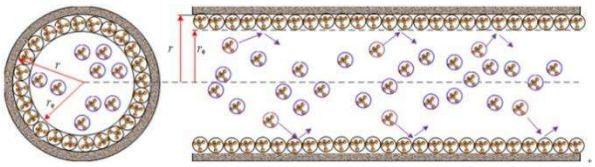

Figure 4. Schematic Diagram of Knudsen Diffusion (Purple arrows represent molecules in Knudsen diffusion)

ISSN: 2414-1895 DOI: 10.6919/ICJE.202501_11(1).0003

$$J_{\text{knudsen}} = -\rho \cdot \frac{D_{\text{k}}}{p} \cdot \nabla p \tag{7}$$

Jknudsen--The mass flow rate of Knudsen diffusion,kg/(m^2·s),

Dk--The Knudsen diffusion coefficient under different capillary diameters,m^2/s,

ρ--the density of gas molecules,kg/m^3.

1.4 Surface Diffusion

Apart from the desorption effect on the micro-nano pore surface of shale gas, surface diffusion also exists, that is, the movement along the adsorption wall. Numerous factors can exert an influence on the surface diffusion of shale, among which include: temperature, pressure, shale gas molecules, the interaction between nanopore wall surfaces, gas molecule attributes, and wall surface properties of shale pores.

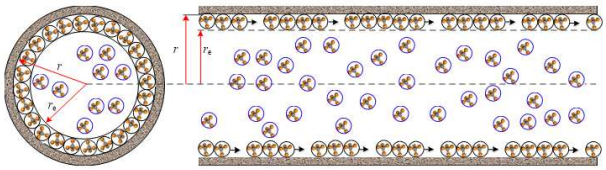

Figure 5. Schematic Illustration of Surface Diffusion (Black arrows represent molecules undergoing surface diffusion)

The mass transport equation of surface diffusion for shale gas:

$$J_{\text{surface}} = -M \cdot D_{\text{s}} \cdot \frac{C_{\text{smax}} p_{\text{L}}}{(p + p_{\text{L}})^2} \cdot \nabla p \tag{8}$$

Jsurface--The surface diffusive mass flow rate,kg/(m^2·s),

Ds--The surface diffusion coefficient,m^2/s,

Csmax--The maximum adsorption concentration of adsorbed gas,mol/m^3,

2. The Comprehensive Apparent Permeability Model of Single Capillary in Shale

The flow of shale gas encompasses viscous flow, slip flow, Knudsen diffusion, desorption of shale gas, and surface diffusion. According to the distinct mass transport equations under diverse conditions and borrowing the approach of introducing contribution coefficients from Adzumi [20] and Mohammad, a comprehensive equation for depicting the migration of shale gas within the shale matrix is established on this foundation.

Considering the viscous flow of free shale gas, slip flow, Knudsen diffusion, desorption of adsorbed gas, and surface diffusion effects, the total transported mass is the superimposition sum of the transported masses resulting from these transport modes. Considering the multiple transport mechanisms of shale gas under multi-scale conditions, substituting equations (4), (5), (6), (7), and (8) into equation (4), the overall mass transport equation can be expressed as:

$$\begin{aligned} J_{\text{tol}} &= (J_{\text{vicious}} + J_{\text{slip}})(1-\varepsilon) + J_{\text{knudsen}} \cdot \varepsilon + J_{\text{surface}} \\ &= -\frac{\rho}{\mu}\left[k_{\text{D}} \cdot (1 - \frac{d_{\text{m}}}{r} \cdot \frac{p}{p + p_L})^2 \cdot F \cdot (1-\varepsilon) + D_{\text{k}} \cdot \frac{\mu}{p} \cdot \varepsilon + M \cdot D_{\text{s}} \cdot \frac{\mu}{\rho} \cdot \frac{C_{\text{smax}} p_L}{(p + p_L)^2} \right] \nabla p \end{aligned} \tag{9}$$

ISSN: 2414-1895 DOI: 10.6919/ICJE.202501_11(1).0003

For the sake of convenience in application, the multi-scale migration model of shale gas can be transformed into the form of an apparent permeability model. By substituting Equation (5), Equation (1) can be expressed as the relationship between the apparent permeability kapp,i of a single capillary and the intrinsic permeability kD as follows:

$$k_{app,i}=k_D\cdot\left[\left(1-\frac{d_m}{r}\cdot\frac{p}{p+p_L}\right)^2+\left(\frac{8\pi RT}{M}\right)^{0.5}\cdot\frac{\mu}{p_{avg}r}\cdot\left(\frac{2}{\alpha}-1\right)\right]\cdot(1-\varepsilon)+\frac{2r}{3}\cdot\left(\frac{8RT}{\pi M}\right)^{0.5}\cdot\frac{\mu}{p}\cdot\varepsilon+M\cdot D_s\cdot\frac{\mu}{\rho}\cdot\frac{C_{smax}p_L}{(p+p_L)^2}$$
$$=k_D\cdot\left[\left(1-\frac{d_m}{r}\cdot\frac{p}{p+p_L}\right)^2+F\right]\cdot(1-\varepsilon)+D_k\cdot\frac{\mu}{p}\cdot\varepsilon+M\cdot D_s\cdot\frac{\mu}{\rho}\cdot\frac{C_{smax}p_L}{(p+p_L)^2} \quad (10)$$

kapp,i--The magnitude of the apparent permeability of the i-th capillary,$10^{-3}\mu m^2$.

It can be discerned from Equation (10) that the apparent permeability of shale is not a constant value but varies with factors such as pore diameter and pressure, meaning that the apparent permeability of shale changes in the actual production process. However, when studying production at present, it is mostly assumed that the permeability is a constant value, and this approach is inappropriate.

For the practical application of Equation (10), the intrinsic permeability of shale, kD, determined through laboratory experiments can be adopted. Then, other parameters in Equation (10) can be corrected by substituting them to obtain the apparent permeability of shale under different pore scales and pressure conditions. It should be noted that when correcting the permeability, pavg and p in Equation (10) are both taken as the pressure values under the correction conditions.

In contrast to the apparent permeability model established by Javadpour [6] et al., the model in this paper incorporates the influence of the surface diffusion term in Xiong's model on mass transfer. Then, drawing on the treatment method of the contribution coefficient by predecessors and considering the viscous flow, slip flow, Knudsen diffusion, desorption of adsorbed gas, and surface diffusion effect of free shale gas, a multi-scale mass transfer equation for the unified flow regime is established.

3. The Permeability Model of Shale Gas Matrix

Due to the previously established visual permeability model of a single capillary for shale gas, which was only used to consider the permeability of shale gas under a single capillary. To describe the magnitude of shale gas permeability at the core scale more accurately, based on the comprehensive visual permeability of shale gas, the pore size of shale gas is analyzed and statistically. The permeability of capillaries under different pore size scales is calculated respectively according to the different distributions of pore size. Then, the pore permeabilities under different pore sizes are superimposed to obtain the permeability magnitude of the entire core [7]. The permeability of shale at the core scale can be calculated according to Equation (11), thereby describing the permeability of shale more accurately.

$$k_{app}=\frac{\phi}{\tau}\sum_{i=1}^{N}k_{app,i}\lambda_i \quad (11)$$

Kapp--Apparent permeability of the matrix,$10^{-3}\mu m^2$,

ϕ --Porosity size, dimensionless,

kapp,i--The magnitude of the apparent permeability of the i-th capillary,$10^{-3}\mu m^2$,

τ --The degree of tortuosity, dimensionless,

λi--The volume fraction of the channel determined based on the porosity distribution, dimensionless.

ISSN: 2414-1895 DOI: 10.6919/ICJE.202501_11(1).0003

$$\tau = 1 - m\ln(\varphi) \tag{12}$$

m--Through the tortuosity fitting parameter, dimensionless, and usually taken as 0.77.

For the Knudsen number of the shale matrix under different capillary tube diameters, it is Kni, dimensionless; the slip coefficient corresponding to the effective flow radius of capillaries of different sizes is Fi, dimensionless; the Knudsen diffusion coefficient corresponding to the effective flow radius of capillaries of different sizes is Dki, m²/s; the contribution coefficient εi corresponding to the effective flow radius of capillaries of different sizes is dimensionless. Then, the apparent permeability of the shale matrix can be calculated by Equation (13).

$$k_{app} = \frac{\varphi}{1 - m\ln(\varphi)} \sum_{i=1}^{n} ((\frac{r_i^2}{8}((1 - \frac{d_m}{r_i} \cdot \frac{p}{p + p_L})^2 + F_i) \cdot (1 - \varepsilon_i) + D_{ki} \cdot \frac{\mu}{p} \cdot \varepsilon_i + M \cdot D_s \cdot \frac{\mu}{\rho} \cdot \frac{C_{s\max} p_L}{(p + p_L)^2}) \cdot \lambda_i) \tag{13}$$

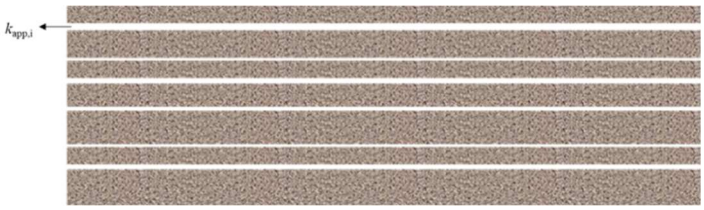

Figure 6. Shale Matrix Seepage under Different Pore Sizes

4. Model Validation

In order to validate the shale gas matrix permeability calculation model established in this paper, the experimental test data of shale matrix permeability obtained through unsteady-state tests were compared and verified. The accuracy of the model in this paper was verified from both the experimental results and the theoretical results. Unsteady-state permeability tests were conducted on four sets of cores respectively. The experimental process is shown in Figure 7. Firstly, the gas source pressurizes the core holder. When the pressure reaches an appropriate value, the gas supply is stopped, and the gas permeates through the downstream chamber from the core [8]. However, during the test process, as the pressure is constantly decreasing, the seepage process is unsteady. Usually, this kind of permeability test method is called the unsteady-state test method [9].

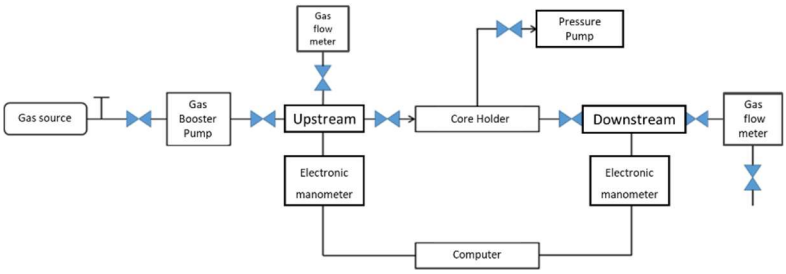

Figure 7. Permeability Testing Process of Shale by Unsteady-State Attenuation Method

The permeability magnitudes of voids at different pore diameters were obtained through calculations, and compared with the permeability results experimentally measured using the permeability model presented in this paper. The permeabilities calculated using this model were: 0.021×10^{-3} μm², 0.011×10^{-3} μm², 0.055×10^{-3} μm², and 0.014×10^{-3} μm²; the permeabilities measured through the non-

ISSN: 2414-1895 DOI: 10.6919/ICJE.202501_11(1).0003

steady-state pressure attenuation method were: 0.019×10^{-3} μm^2, 0.010×10^{-3} μm^2, 0.051×10^{-3} μm^2, and 0.012×10^{-3} μm^2. During the process of measuring the core permeability in the laboratory, the non-steady-state pressure attenuation method was employed to determine the permeability of the shale matrix. Considering the significant slip effect of the shale matrix, the surface diffusion of gas was not taken into account. Consequently, the permeabilities obtained through the model in this paper were significantly greater than those measured in the laboratory. To eliminate the error caused by surface diffusion in increasing the permeability, the magnitudes of the core permeability without considering surface diffusion were: 0.020×10^{-3} μm^2, 0.0099×10^{-3} μm^2, 0.053×10^{-3} μm^2, and 0.013×10^{-3} μm^2. Through comparison, it was discovered that the errors between the permeabilities calculated using the model considering surface diffusion and desorption and those measured using the non-steady-state method for the four sets of cores were approximately 9.5%, 10.1%, 8.6%, and 12.3%, respectively. If surface diffusion and desorption were not considered when calculating the permeability using the model in this paper, the errors between the two were reduced to 4.7%, 5.2%, 4.7%, and 3.5%. Therefore, the calculation accuracy of the model presented in this paper is relatively high.

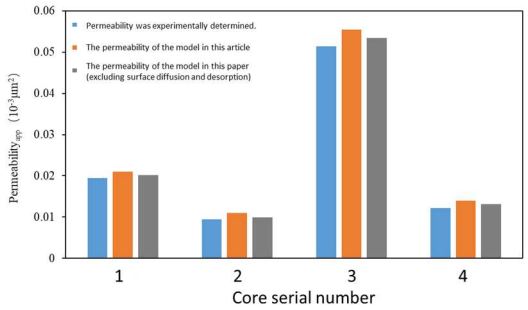

Figure 8. The Permeability Magnitudes of Pores at Different Pore Diameters

5. Conclusion

(1) By introducing weighted coefficients and comprehensively considering multiple transport mechanisms such as the viscous flow of free shale gas, Knudsen diffusion, slip effect, desorption of adsorbed shale gas, and surface diffusion, a unified multi-scale transport model of shale gas was established for the first time. This model can uniformly calculate the mass transfer equations of different flow states. Through comparisons with experimental data and classic theoretical models, the correctness and comprehensiveness of this model were verified. Compared with the classic theoretical model by Javadpour, the influence of surface diffusion on the apparent permeability was taken into account in this model, making it more applicable.

(2) The apparent permeability of shale at the nano-micro scale is affected by the properties of reservoir rocks, gas properties, seepage temperature, and pressure conditions. Among them, the influences of temperature and the molecular mass of gas are relatively small, while the pore scale and pressure changes have a greater impact on the microscopic transport mechanism. As the pore scale decreases and the pressure drops, the apparent permeability of shale increases.

Therefore, the apparent permeability model of the shale matrix in this paper can make up for the deficiencies in the non-steady-state testing process of the shale matrix, considering the influences of factors such as temperature, pressure, and the transport of adsorbed gas on the permeability of the shale matrix.

References

[1] Adzumi. Studies on the flow of gaseous mixtures through capillaries. II. the molecular flow of gaseous mixtures[J]. Bulletin of the Chemical Society of Japan, 1937, 12(6):285-291.

ISSN: 2414-1895 DOI: 10.6919/ICJE.202501_11(1).0003

[2] Singh H, Javadpour F, Ettehadtavakkol A, et al. Nonempirical apparent permeability of shale[J]. SPE Reservoir Evaluation & Engineering. 2013, 17(3): 414-424.

[3] Guo Xiao, Zhang Mengli, Liu Hong. Multi-scale Porous Medium Visual Permeability Model[J]. Applied Petrochemical Technology, 2016, 04(5): 18-22.

[4] Deng J, Zhu W, Ma Q. A new seepage model for shale gas reservoir and productivity analysis of fractured well[J]. Fuel, 2014, 124(15):232-240.

[5] Shi, L Z, Li. Diffusion and flow mechanisms of shale gas through matrix pores and gas production forecasting[C]. SPE Paper 167226 presented at SPE Unconventional Resources Conference Canada, Calgary, Alberta, Canada, 2013

[6] Javadpour, Fisher, Unsworth. Nanoscale gas flow in shale gas sediments[J]. Journal of Canadian Petroleum Technology, 2007, 46(10):55-61.

[7] Kazemi M, Takbiri-Borujeni A. An analytical model for shale gas permeability[J]. International Journal of Coal Geology, 2015,146(05):188-197.

[8] Luo Yi. Unsteady Evaluation Method for Seepage Capacity of Shale Reservoirs [D]. Chengdu: Chengdu University of Technology, 2016.

[9] Yu Rongze, Bian Yana, Zhang Xiaowei, et al. A Review on Non-Steady-State Permeability Test Methods for Shale Reservoirs [J]. Science Technology and Engineering, 2012, 05(27): 7019 - 7027.